UJEAS

UNIZIK JOURNAL OF ENGINEERING AND APPLIED SCIENCES

UNIZIK Journal of Engineering and Applied Sciences 6(4), December (2026), 3999-4010
Journal homepage: https://journals.unizik.edu.ng/index.php/ujeas
PRINT ISSN: 2992-4383 || ONLINE ISSN: 2992-4391

ETAP-Based Design and Reliability Assessment of a Smart 33/11 kV Injection Substation

[1]Kelvin Kanayo Eze, [*2]Ugochukwu Edebeani Anionovo, [3]Charles Austeen Ibe, [4]Obinna Chika Ikaraoha, [5]Emmanuel Aninye Anazia
[,2,4,5]Electrical Engineering Department, Nnamdi Azikiwe University, Awka, Anambra State.
[3]Forensic Science Department, Nnamdi Azikiwe University, Awka, Anambra State.

*Corresponding Author's E-mail: ue.anionovo@unizik.edu.ng

Abstract
Medium-voltage injection substations are critical interfaces between transmission supply and distribution feeders, yet many networks in developing power systems continue to experience feeder overloading, voltage-profile deterioration, limited operational visibility, and weak contingency margins. This paper presents an ETAP-based design and assessment of a smart 33/11 kV injection substation using the Agu Awka Injection Substation in Anambra State, Nigeria, as the study system. A detailed network model comprising two 15 MVA, 33/11 kV transformers, a 625 kVA auxiliary transformer, two 33 kV grid in-feeds, an 11 kV busbar, and four outgoing feeders was developed. The proposed smart architecture incorporates supervisory control and data acquisition, intelligent electronic devices, automated switching/reclosing, smart fault indicators, online transformer condition monitoring, edge computing, weather sensing, and a smart remote terminal unit. Newton–Raphson load-flow analysis, multi-fault short-circuit analysis, and N-1/N-2 contingency screening were performed. The base case converged with zero active- and reactive-power mismatch. The network demand was 18.467 MW and 6.070 Mvar, while total losses were 0.277 MW and 1.958 Mvar. The four outgoing feeders operated at approximately 102.7–103.1% of their stated ratings, while the two 33 kV sources operated at 91.92% power factor. The highest reported symmetrical fault level occurred at the 0.415 kV auxiliary bus (22.718 kA), while the 11 kV Bus6 recorded approximately 16.279 kA for the three-phase fault case. Contingency screening identified Bus6 as the most severe N-1 event and showed that the network has little practical N-2 capacity, with surviving transformers reaching approximately 431% loading in severe cases. The results indicate that digital monitoring and automation should be implemented together with physical capacity reinforcement, reactive-power compensation, and an alternative 11 kV supply path. The study provides a practical simulation framework for modernization of medium-voltage injection substations in developing-country distribution networks.
Keywords: Smart Substation, Injection Substation, ETAP, Distribution Automation, Load flow, Short-circuit Analysis, Contingency Analysis, IEC 61850, Agu Awka.

1. Introduction

Electrical distribution systems are essential to industrial activity and everyday life. Injection substations form a key interface in this system by receiving power at a higher voltage, stepping it down for distribution, and providing the switching, protection, measurement, and control functions needed to keep feeders in service. In many developing power systems, however, these functions still depend heavily on manual operation, limited monitoring, fixed protection settings, and slow fault localization. The result can be repeated feeder outages, declining voltage quality, technical losses, equipment overloading, and longer restoration times (Chen et al., 2023; Moradi-Sepahvand et al., 2023).

Substation digitalization offers a practical route from largely reactive operation to more visible, data-driven, and automated control. A smart substation brings together Intelligent Electronic Devices (IEDs), supervisory control and data acquisition (SCADA), remote terminal units (RTUs), networked sensors, digital protection, automated switching, and standardized communications. IEC 61850 is central to this approach because it provides common information models and communication services that allow substation devices to work together (IEC 61850-7-2, 2020; IEC 61850-8-1, 2020). These capabilities can improve operational visibility, shorten fault-response time, and support condition-based asset management (Girdhar et al., 2024; Heluany and Gkioulos, 2024).

Simulation is particularly important when a conventional substation is being considered for modernization because changes in topology, loading, protection, and equipment configuration have to be assessed before they are implemented. ETAP provides integrated tools for load flow, short-circuit, contingency, protection, and related distribution studies. This makes it possible to assess the electrical consequences of the proposed upgrade within one consistent network model.

A gap remains in studies that bring these electrical and digital considerations together for a practical medium-voltage injection substation in a developing-country setting. Existing work often concentrates on a single issue—such as communication reliability, cybersecurity, adaptive protection, distributed generation, or predictive maintenance—without assessing the electrical network and the smart-substation layer as one system. This paper addresses that gap through an ETAP-based case study of the Agu Awka 33/11 kV injection substation. The work models the existing network, develops a smart-substation architecture, evaluates steady-state performance, examines fault duty, and tests network resilience under N-1 and N-2 contingencies. Figure 1 presents the conceptual transition adopted for the proposed modernization.

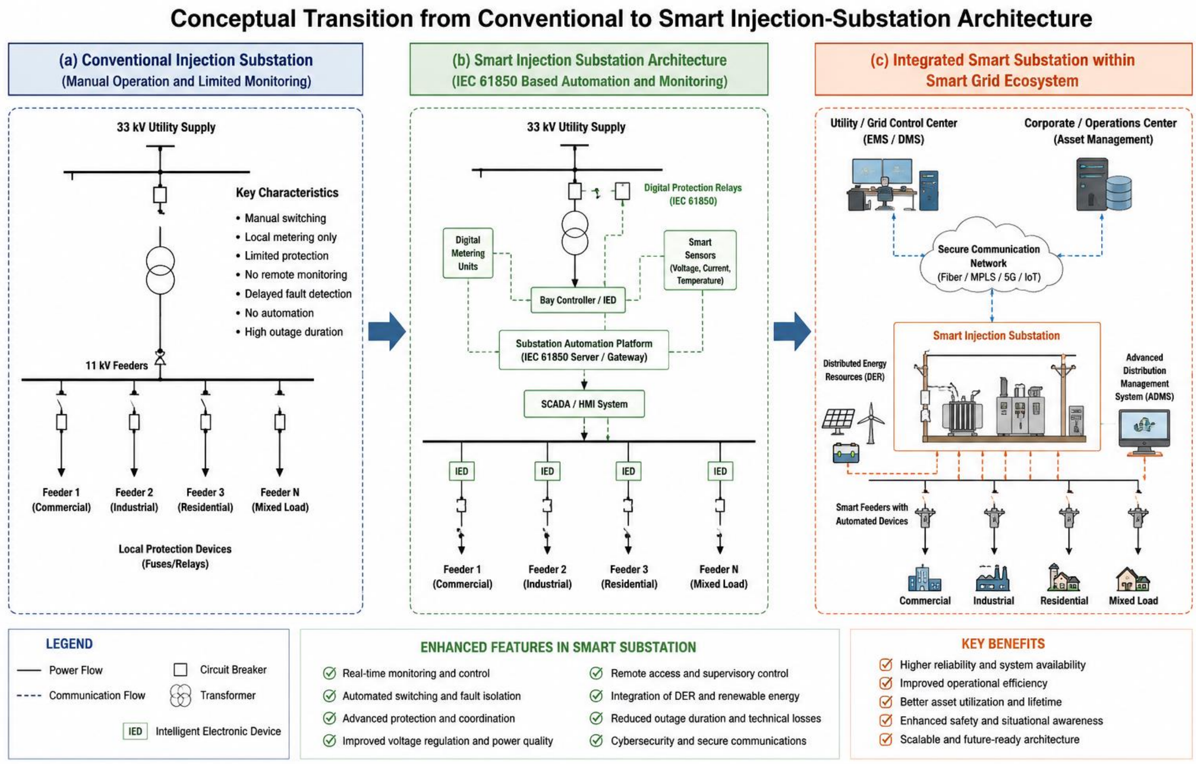

Fig. 1. Conceptual transition from conventional to smart injection-substation architecture.

Figure 1: Conceptual transition from conventional to smart injection-substation architecture. (Source: Authors' conceptual design; AI-assisted visualization).

1.1. Smart Substation Architecture

A smart substation extends the conventional substation by adding sensing, local processing, communications, and coordinated control. The commonly adopted process, bay, and station levels provide a useful way of organizing these functions. At the process level, electrical quantities are acquired from instrument transformers or non-conventional sensors and converted into digital information. At the bay level, IEDs perform protection, control, measurement, and event-recording functions. The station level provides operator interfaces, data storage, supervisory control, and communication with the wider control centre (IEC 61850-7-2, 2020; IEC 61850-8-1, 2020; Zhu et al., 2023).

For Agu Awka, this architecture is intended to provide better visibility of feeder and transformer conditions without suggesting that communication equipment can replace physical network reinforcement. The proposed layer includes automated breakers/reclosers, feeder fault indicators, transformer condition monitoring, an RTU/SCADA interface, weather sensing, and local edge processing. Together, these functions can reduce the time required to detect, locate, and respond to suitable faults while providing operators with better information for switching and maintenance decisions.

1.2 IEC 61850 and Digital Substation Communication

IEC 61850 provides the communication and information-model foundation for interoperable digital substations. Its logical-node model allows functions such as measurement, protection, and tripping to be represented in a standardized form. For the proposed architecture, Sampled Values (SV) are assigned to high-speed streams of digitized current and voltage measurements at the process level, while Generic Object-Oriented Substation Event (GOOSE) messages provide fast peer-to-peer exchange of protection and control signals between IEDs. Manufacturing Message Specification (MMS) is suited to station-level supervisory functions, including monitoring, reporting, and data exchange with higher-level systems (IEC 61850-7-2, 2020; IEC 61850-8-1, 2020). The literature also shows that communication reliability and cybersecurity are now integral parts of digital-substation design. Redundant communication paths can improve fault tolerance, while secure architectures and monitoring are needed to reduce exposure to communication disruption, false-data injection, and unauthorized access (Mathebula and Saha, 2022; Husnoo et al., 2023; Girdhar et al., 2024). These considerations are relevant to Agu Awka because the proposed digital layer will depend on continuous and trustworthy measurements for protection, monitoring, and supervisory decisions.

1.3 Power-System Studies for Substation Assessment

Load-flow analysis provides the steady-state picture needed to judge whether buses, feeders, and transformers are operating within acceptable limits. It gives the voltage magnitude and phase angle at buses, active and reactive power flows, losses, and equipment loading. Newton–Raphson is widely used because of its convergence and numerical accuracy, although the suitability of any load-flow method depends on the network and study objective (Glover et al., 2017).

Short-circuit analysis complements load flow by establishing the fault-current levels that equipment and protection systems must withstand and interrupt. Three-phase, line-to-ground, line-to-line, and double-line-to-ground faults are commonly considered. For this study, the time behaviour of the fault current is also relevant because the asymmetrical peak and the persistence of the dc component can affect breaker duty and equipment withstand requirements.

Contingency analysis then tests what happens when important network elements are lost. N-1 represents the loss of one element, while N-2 represents the simultaneous loss of two elements. In a network such as Agu Awka, where two main transformers and four feeders share a common 11 kV bus, contingency analysis is especially useful for identifying single points of failure and revealing how quickly spare capacity is exhausted.

1.4 Smart Monitoring, Edge Computing, and Cybersecurity

Smart monitoring adds value when the information collected at the substation can be turned into timely operating decisions. Edge computing is particularly attractive for this purpose because basic data-quality checks, filtering, event detection, and alarm generation can be performed close to the equipment rather than sending every raw measurement to a remote server. Recent work on distribution automation and digital substations points to edge processing as an important enabler of responsive monitoring and control (Zhu et al., 2023).

At the same time, increased connectivity creates new cyber-physical risks. False-data injection, communication spoofing, denial-of-service attacks, and unauthorized access can compromise the reliability of automated decisions. Cybersecurity therefore needs to be considered alongside the electrical and communication design rather than added as an afterthought (Husnoo et al., 2023; Girdhar et al., 2024; Roomi et al., 2025).

1.5 Empirical Studies and Research Gap

Previous studies provide useful evidence for the individual technologies considered in this work. Mathebula and Saha (2022), for example, showed the reliability benefits of redundant IEC 61850 communication architectures. Cabral et al. (2026) examined digital-substation modelling and safety using IEC 61850, while Girdhar et al. (2024) investigated software-defined approaches to cyber restoration. Other studies have addressed active distribution-system control, distributed generation, cybersecurity, digital twins, and ETAP-based network analysis (Chen et al., 2023; El-Fergany, 2024; Heluany and Gkioulos, 2024).

The limitation of this body of work, from the perspective of the present case study, is that these issues are often treated separately. The contribution of this paper is therefore not a new communication protocol or a new load-flow algorithm; rather, it is the integration of electrical performance assessment, contingency screening, short-circuit duty, and a practical smart-substation architecture around an actual 33/11 kV injection-substation model. The approach also makes the distinction between what has been demonstrated by simulation and what remains to be validated in the field.

2.0 Materials and methods

2.1 Study Network

The study system is the Agu Awka 33/11 kV injection substation in Anambra State, Nigeria. It is supplied by two 33 kV grid in-feeds and uses two 15 MVA, 33/11 kV transformers as the main sources to the 11 kV bus. A 625 kVA, 33/0.415 kV transformer supplies auxiliary services. The 11 kV section feeds the Amansea, Ifite, Industrial, and Unizik feeders. The ETAP model includes the buses, transformers, feeders/cables, circuit breakers, instrument transformers, protection elements, and loads represented in the available network data.

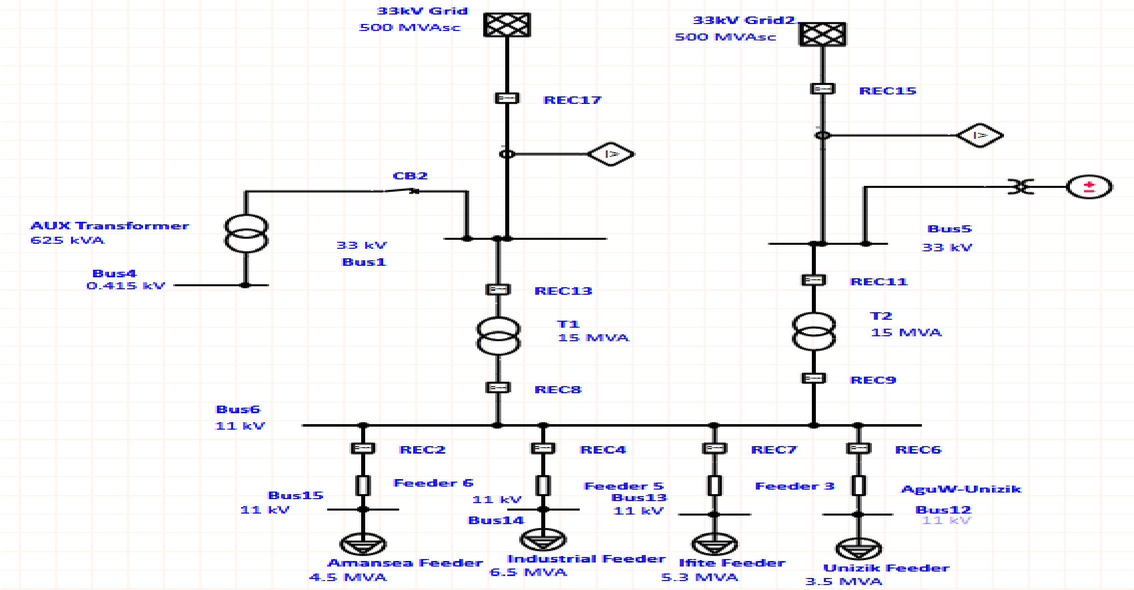

Figure 2: ETAP Agu Awka 33/11 kV single-line diagram

2.2 Smart-Substation Configuration

The proposed upgrade adds a digital and automation layer to the existing electrical arrangement rather than treating digitalization as a substitute for reinforcement. The concept includes automated reclosing, feeder fault indication, online transformer condition monitoring, an RTU/SCADA interface, weather sensing, and local edge processing. The intention is to improve visibility, fault localization, switching, restoration, and asset monitoring while leaving room for future adaptive protection and distributed-energy-resource integration.

2.3 Input Data and Simulation Procedure

The model inputs comprised bus voltage levels, feeder impedances, transformer ratings, feeder configurations, load demands, protection-device information, breaker ratings, and power-factor data. Where utility records were not available, the thesis used standard engineering references, ETAP library parameters, manufacturer information, and typical Nigerian 11/33 kV distribution values. The simulation workflow was: (1) construct the one-line model; (2) enter and check network parameters; (3) solve the Newton–Raphson load flow; (4) perform short-circuit studies for the specified fault types; and (5) screen N-1 and N-2 contingencies.

Table 1: Principal modeled equipment, feeders, and bus voltage levels.

Equipment / Feeder	Bus / Voltage	Rating / Capacity	Length	Cable / Conductor	Allowable Ampacity	Function / Note
33 kV Grid Source 1	Bus1 / 33 kV	500 MVA	—	—	—	Grid source
33 kV Grid Source 2	Bus5 / 33 kV	500 MVA	—	—	—	Grid source
Transformer T1	Bus1–Bus6	15 MVA, 33/11 kV	—	—	—	Main power transformer
Transformer T2	Bus5–Bus6	15 MVA, 33/11 kV	—	—	—	Main power transformer
Auxiliary Transformer	Bus1–Bus4	625 kVA, 33/0.415 kV	—	—	—	Station auxiliary supply
Unizik Feeder	Bus6–Bus12 / 11 kV	3,500 kVA load rating	0.80 km	1 × 3/C 240 mm²	302 A	11 kV outgoing feeder
Ifite Feeder	Bus6–Bus13 / 11 kV	5,300 kVA load rating	1.20 km	1 × 3/C 240 mm²	302 A	11 kV outgoing feeder
Industrial Feeder	Bus6–Bus14 / 11 kV	6,500 kVA load rating	1.50 km	1 × 3/C 400 mm²	378.6 A	11 kV outgoing feeder
Amansea Feeder	Bus6–Bus15 / 11 kV	4,500 kVA load rating	1.50 km	1 × 3/C 240 mm²	302 A	11 kV outgoing feeder

Bus voltage – Bus1	33 kV	—	—	—	—	Grid/source bus
Bus voltage – Bus5	33 kV	—	—	—	—	Grid/source bus
Bus voltage – Bus6	11 kV	—	—	—	—	Main distribution bus
Bus voltage – Bus12	11 kV	—	—	—	—	Unizik feeder terminal
Bus voltage – Bus13	11 kV	—	—	—	—	Ifite feeder terminal
Bus voltage – Bus14	11 kV	—	—	—	—	Industrial feeder terminal
Bus voltage – Bus15	11 kV	—	—	—	—	Amansea feeder terminal
Bus voltage – Bus4	0.415 kV	—	—	—	—	Auxiliary-service bus

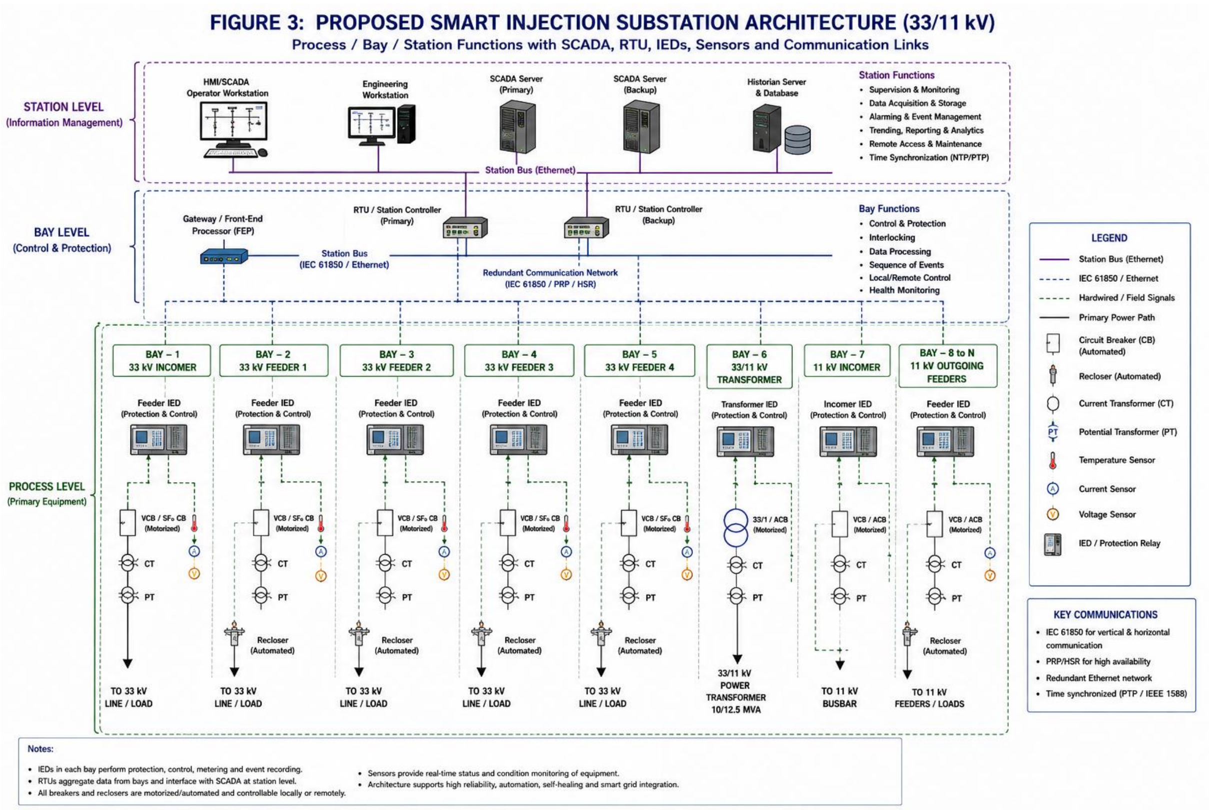

Figure 3: Proposed smart-substation architecture showing process, bay, and station functions, SCADA, RTU, IEDs, sensors, automated breakers/reclosers, and communication links. (Source: Authors' conceptual design; AI-assisted visualization.)

2.4 Field Validation and ETAP Model Calibration

The original study was constrained by limited access to time-stamped utility operating data. To make this limitation explicit and provide a reproducible validation path, the ETAP model should be checked against SCADA or substation meter records for a representative operating period before the model is used for investment decisions. The comparison should use matched time stamps and the same network topology in both datasets.

The recommended validation set includes 33 kV source voltage, current, active and reactive power, and power factor; 11 kV Bus6 voltage and current; individual feeder current and power; transformer loading; breaker status; and relevant alarms or events. For each quantity available in both datasets, the comparison should report absolute error and percentage error, with MAE, RMSE, and MAPE used where appropriate. Parameters that remain uncertain—such as feeder impedance, transformer impedance, or load allocation—can then be calibrated within defensible engineering ranges and the calibrated model checked against a separate SCADA period. No field-validation result is claimed here because the required time-synchronized utility dataset was not available for this manuscript.

2.5 Proposed IEC 61850 Communication and Edge-Processing Specification

The proposed digital layer is organized around the IEC 61850 process, bay, and station levels. SV is intended for process-level current and voltage streams from merging units; GOOSE is intended for fast peer-to-peer protection and interlocking signals between IEDs; and MMS is intended for station-level monitoring, reporting, configuration, and supervisory data exchange (IEC 61850-7-2, 2020; IEC 61850-8-1, 2020; IEC TR 61850-90-4, 2020). IEEE 1588 Precision Time Protocol is proposed for time synchronization so that events from different devices can be compared on a common time base.

For planning purposes, the station backbone is specified as a managed 1 Gb/s fibre-optic Ethernet network, with access links of at least 100 Mb/s to field devices where the device interfaces permit. VLAN segmentation, traffic prioritization, redundant paths for critical protection traffic, and controlled access between process, bay, and station networks are proposed to improve availability and security. These are design specifications for the proposed architecture, not measured characteristics of the existing Agu Awka installation.

The edge node is intended to perform lightweight processing before information is forwarded to the control centre. The proposed sequence is: data-quality and timestamp checks; moving-window filtering; RMS/phasor calculation where required; threshold and rate-of-change checks; feeder-overload detection; transformer-condition trend checks; event classification; and alarm/event generation. The processing layer is therefore intended to support operators with timely, locally generated information rather than replace the protection functions of dedicated IEDs.

2.6 Performance Metrics

The assessment considered voltage profile, active and reactive losses, feeder and transformer loading, short-circuit current, transient DC-component behavior, and contingency severity. Reliability interpretation focused on outage tolerance, supply-path redundancy, and the network's ability to accommodate component loss without unacceptable voltage or thermal violations.

3.0 Result and Discussion

3.1 Base-Case Load Flow

The normal load-flow solution converged with zero MW and Mvar mismatch. The modeled demand was 18.467 MW and 6.070 Mvar, supplied by the two 33 kV sources at 18.744 MW and 8.028 Mvar. The resulting network losses were 0.277 MW and 1.958 Mvar. The active-power loss is about 1.5% of the modeled source power, while the comparatively larger reactive loss is consistent with the inductive characteristics of the feeders and transformers.

Voltage declined gradually from the 33 kV source buses toward the 11 kV feeder terminals. Bus6 was at 96.21% of nominal voltage, while the feeder terminals ranged from 95.21% to 95.80%. The lowest terminal voltage was 95.21% at Amansea, followed closely by 95.22% at Industrial. Thus, the base case remained within the ±5% voltage band used in the thesis, although the downstream decline shows that the longer and more heavily loaded feeders have less voltage margin.

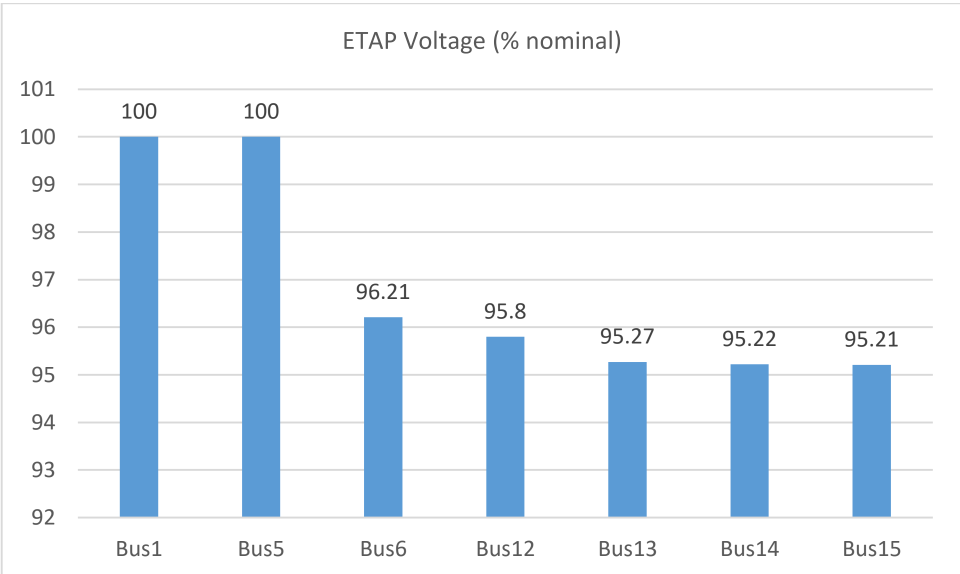

Figure 4: Base-case bus-voltage profile (% nominal) from Bus1/Bus5 through Bus6 and feeder buses Bus12–Bus15.

Table 2: Base-Case Load-Flow Summary of the Agu Awka 33/11 kV Injection Substation.

Bus ID	Nominal kV	Voltage (%)	MW	Mvar	Current (A)	Loading (% of applicable rating)
Bus1	33	100.00	9.372	4.014	178.4	67.9795301
Bus4	0.415	100.00	0.000	0.000	0.0	0
Bus5	33	100.00	9.372	4.014	178.4	67.9795301
Bus6	11	96.21	18.620	6.175	1070.0	67.95412668
Bus12	11	95.80	3.270	1.075	188.6	102.6660744
Bus13	11	95.27	4.942	1.624	286.6	103.0276109
Bus14	11	95.22	6.060	1.992	351.6	103.0596877
Bus15	11	95.21	4.195	1.379	243.4	103.053174

Note: Bus6 loading is referenced to the combined 30 MVA capacity of T1 and T2, whereas the feeder values are referenced to the individual feeder load ratings represented in ETAP. These are different rating bases and therefore should not be compared as if they used the same denominator. A separate cable-ampacity cross-check gives approximately 62.5–94.9% for Unizik, Amansea, Industrial, and Ifite, respectively.

3.2 Feeder and Transformer Loading

The four outgoing feeders were highly utilized on the feeder load-rating basis reported by the ETAP model: Amansea, Ifite, Industrial, and Unizik were at 103.1%, 103.0%, 103.1%, and 102.7%, respectively. This does not mean that every physical cable is operating above its thermal ampacity. The separate branch/cable check places the cable utilization at approximately 80.6% for Amansea, 94.9% for Ifite, 92.9% for Industrial, and 62.5% for Unizik. The distinction resolves the apparent mismatch between the feeder loading percentages and the physical cable ratings and shows that the most immediate concern is feeder capacity on the stated load-rating basis, with Ifite and Industrial also closest to their cable ampacity limits.

Transformers T1 and T2 were each at 68% loading in the normal case. Each transformer showed an estimated 3.79% voltage drop and losses of about 61.75 kW and 926.2 kvar. The base case therefore does not show a uniform overload across the substation: the feeder circuits are the tighter steady-state constraint, while transformer capacity becomes critical when an outage forces more load through the remaining supply path.

Table 3. Feeder and Transformer Loading Comparison (with Cable-Ampacity Cross-Check)

Equipment	Rating (kVA/MVA)	MW	Mvar	Current (A)	Power Factor (%)	Loading (%)	Terminal Voltage (%)	Active Loss (kW)	Reactive Loss (kvar)	Cable Ampacity Cross-Check (%)
Amansea Feeder	4,500 kVA	4.195	1.3788	243.4	95.0	103.1	95.21	40.91	24.00	80.6
Ifite Feeder	5,300 kVA	4.9419	1.6243	286.6	95.0	103.0	95.27	45.36	26.61	94.9
Industrial Feeder	6,500 kVA	6.0598	1.9918	351.6	95.0	103.1	95.22	54.07	47.23	92.9
Unizik Feeder	3,500 kVA	3.2703	1.0749	188.6	95.0	102.7	95.80	13.10	7.68	62.5
Transformer T1	15 MVA, 33/11 kV	9.3720	4.0139	178.4	91.92	68.0	96.21	61.75	926.20	—
Transformer T2	15 MVA, 33/11 kV	9.3720	4.0139	178.4	91.92	68.0	96.21	61.75	926.20	—

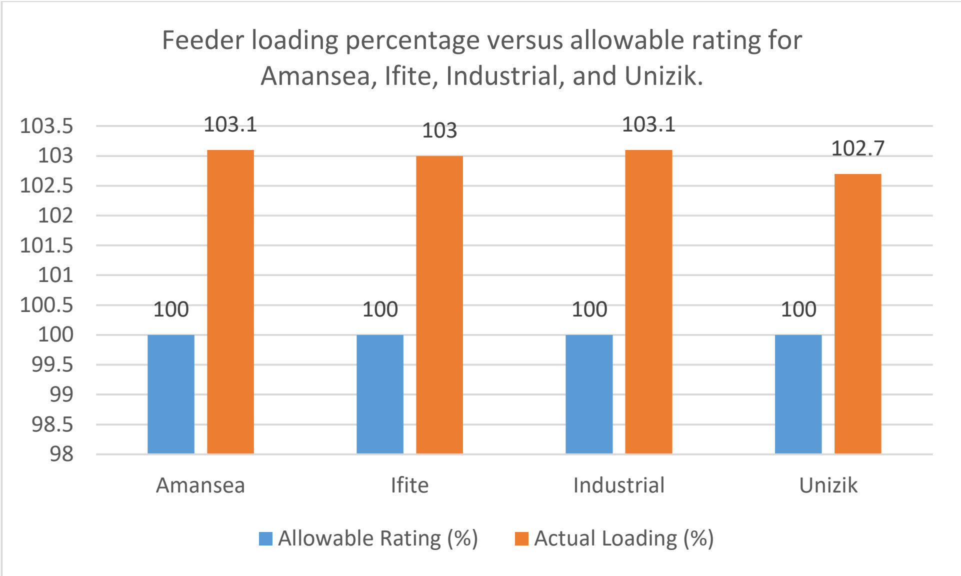

Figure 5: Feeder loading percentage versus allowable rating for Amansea, Ifite, Industrial, and Unizik.

3.3 Source Power Factor

The two 33 kV sources shared the modeled load approximately equally, each supplying 9.372 MW and 4.014 Mvar. Their power factor was 91.92%. This value is below the approximately 95% target adopted in the thesis discussion and indicates a reactive-power requirement that can be addressed through appropriately sized compensation, subject to a detailed voltage and harmonic assessment.

3.4 Short-Circuit Performance

Short-circuit analysis considered three-phase, line-to-ground, line-to-line, and line-to-line-to-ground faults. The 33 kV source buses had initial symmetrical three-phase fault currents of about 10.151–10.153 kA. The highest symmetrical fault current in the modeled system occurred at the 0.415 kV auxiliary bus (22.718 kA), while Bus6 recorded 16.279 kA for the three-phase case. The higher Bus6 fault level is consistent with its electrical proximity to the two 15 MVA transformers operating in parallel.

The transient results also show why breaker duty should not be judged from symmetrical RMS current alone. Bus5 and Bus6 retained comparatively persistent dc components, whereas Bus4 had the largest fault-current magnitude but a faster decay. At about 0.1 s, Bus5 retained roughly 10–12% of the plotted initial dc component and Bus6 still had a measurable component. These results define the fault-duty envelope that should be considered in subsequent protection and switchgear verification.

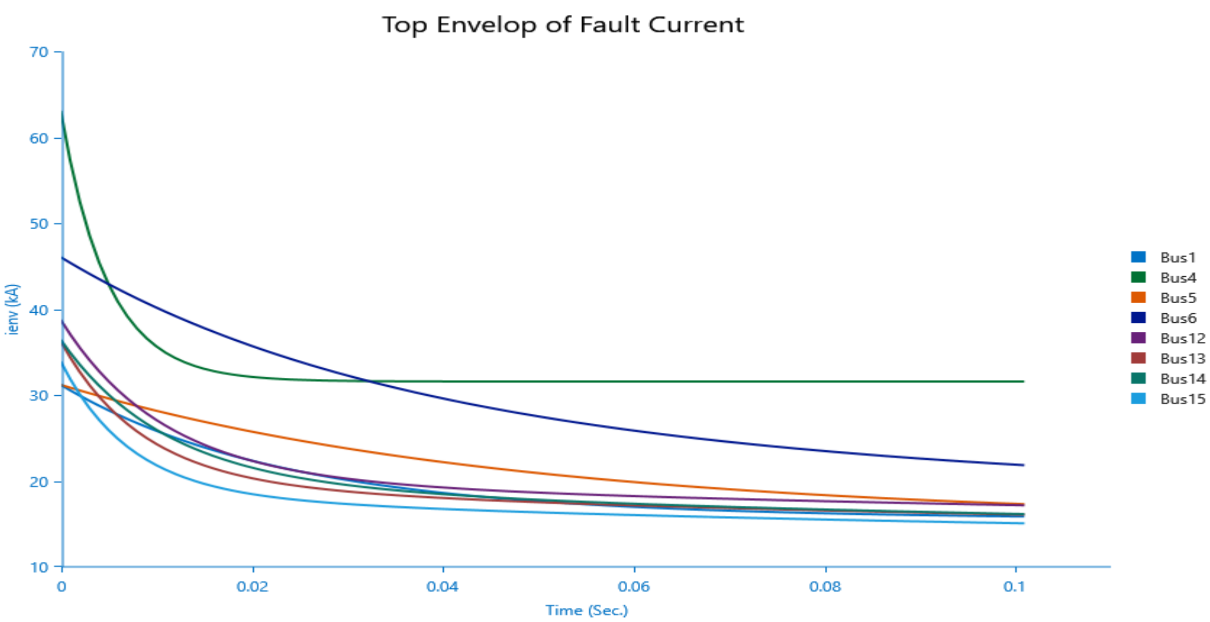

Figure 6: ETAP short-circuit current envelope for critical buses, showing initial asymmetrical peak and decay over the simulation interval.

TABLE 4. Short-Circuit Summary by Critical Bus and Fault Type

Critical Bus	Nominal kV	Three-Phase (I'') (kA)	L-G (I'') (kA)	L-L (I'') (kA)	L-L-G (I'') (kA)	Peak Current, Method C (kA)	DC-Component Observation
Bus1	33	10.1506	9.6356	8.7907	9.9393	24.07	Moderately slow decay; measurable DC component persists beyond 0.05 s
Bus4	0.415	22.7184	22.9219	19.6747	22.9068	37.61	Fastest decay; DC component approaches zero within approximately 0.02–0.03 s
Bus5	33	10.1532	9.6438	8.7929	9.9256	26.09	Slowest decay; approximately 10–12% of the initial plotted value remains at 0.1 s
Bus6	11	16.2787	17.5228	14.0978	17.0583	43.72	Persistent DC offset; approximately 9% of the peak AC component remains at 0.1 s

3.5 Protection Coordination and Breaker-Duty Verification

The short-circuit study establishes the fault-current levels needed for protection and switchgear design, but it does not by itself demonstrate relay coordination. A complete coordination study requires the actual relay models and settings, including CT ratios, pickup currents, time-current characteristics, time-dial or curve parameters, breaker operating times, and the manufacturer interrupting and short-time withstand ratings. Those verified data were not available in the source material, so relay time-overcurrent (TOC) curves and breaker-adequacy claims are not presented as completed results in this paper.

The simulated fault levels should instead be treated as the duty envelope for the next design stage. In particular, the reported three-phase currents and asymmetrical peaks at Bus4, Bus5, and Bus6 should be compared with the interrupting, momentary, and short-time ratings of the installed breakers. The protection study should then plot the upstream and downstream relay curves for the relevant feeder and transformer fault paths and verify grading margins for the normal, N-1, and future distributed-generation configurations.

3.6 Contingency Analysis

The contingency study screened fifteen major network elements individually and in pairwise combinations. ETAP identified 13 non-trivial N-1 cases and 101 N-2 combinations that produced violations. A combined severity index was calculated from the voltage-violation and branch-loading severity scores. Loss of Bus6, the common 11 kV busbar, was the most severe N-1 event with a combined index of 279.76, followed by loss of Bus1 with an index of 102.65.

The contingency results expose the network's limited spare capacity. Under severe contingency combinations, T1 and T2 reached approximately 431% of rated loading, while the auxiliary transformer reached approximately 1,443%. T1 and T2 were flagged in 11 of the 13 non-trivial N-1 cases and in 66 and 62 of the 101 N-2 combinations, respectively. The auxiliary transformer was flagged in 10 N-1 cases and 66 N-2 combinations. The practical implication is clear: the base network can tolerate selected single outages, but it has very little useful N-2 margin.

Table 5. Ranked N-1 Contingency Results

Rank	Outaged Element(s)	Contingency Type	Voltage Severity Score (VVsp)	Branch-Loading Severity Score (SSsp)	Combined Severity Index
1	Bus6 (11 kV busbar)	Bus outage	250.00	29.76	279.76
2	Bus1 (33 kV Grid 1 in-feed)	Bus / grid-source outage	100.00	2.65	102.65
3	AguW–Unizik cable; Bus12, Bus13, Bus14, Bus15; Feeder 3, Feeder 5, Feeder 6	Cable / bus / feeder outage *(eight elements tied)*	50.00	35.07	85.07
4	Bus5 (33 kV Grid 2 in-feed)	Bus / grid-source outage	50.00	32.42	82.42
5	Auxiliary transformer / Bus4	Transformer / bus outage	50.00	5.31	55.31

Table 6. Critical Branch-Loading Alerts Under N-1/N-2 Contingencies

Branch	Type	Flagged Post-Contingency Loading (% of Rating)	N-1 Cases in Violation (of 13)	N-2 Combinations in Violation (of 101)
T1	33/11 kV transformer	≈431%	11	66
T2	33/11 kV transformer	≈431%	11	62
Auxiliary Transformer	33/0.415 kV transformer	≈1,443%	10	66

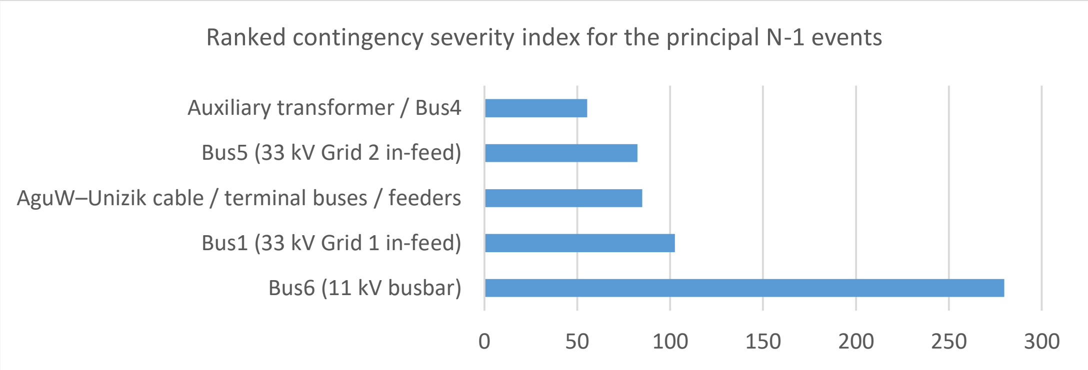

Figure 7: Ranked contingency severity index for the principal N-1 events.

3.7 DISCUSSION

The results demonstrate that the Agu Awka substation's principal challenge is not a single operating deficiency but the interaction of feeder thermal stress, reactive-power demand, voltage-margin reduction, and limited redundancy. Under normal conditions, the system remains within the voltage band and the transformers have substantial thermal headroom. However, the feeder circuits are already operating at or slightly above their stated ratings. Consequently, the apparent adequacy of the transformer capacity in the base case should not be interpreted as evidence of strong contingency resilience.

Bus6 is a particularly important reliability point because both 33/11 kV transformers feed the four outgoing feeders through the same 11 kV busbar. Its loss therefore removes the common supply interface to the distribution feeders. The contingency ranking quantitatively confirms this single-point-of-failure characteristic. This finding supports the broader principle that automation should be coupled with network reconfiguration and redundancy; digital visibility alone cannot restore power when no alternative electrical path exists.

The smart-substation functions proposed in this article are therefore best understood as operational-enabling measures. Automated reclosers can reduce restoration time for suitable transient faults; feeder fault indicators can reduce fault-location time; online transformer monitoring can identify emerging thermal or insulation problems; and an RTU/SCADA layer can improve system visibility and remote control. IEC 61850-based communication can provide an interoperable platform for IED data exchange and high-speed event signaling (IEC 61850-7-2, 2020; IEC 61850-8-1, 2020). These capabilities are consistent with the literature emphasizing digital substations, automation, and intelligent monitoring (Cabral et al., 2026; Girdhar et al., 2024; Ratshitanga et al., 2023).

Nevertheless, the simulation also establishes a critical engineering boundary which states that automation cannot compensate for inadequate physical capacity. A network that reaches several hundred percent transformers loading under a credible double outage requires reinforcement, an alternative supply path, or coordinated load shedding/transfer. Similarly, the 91.92% source power factor supports a case for reactive-power compensation, but the size and location of compensation should be determined through a dedicated optimization and harmonic assessment rather than assumed from the present load-flow result.

The short-circuit results provide a second design implication. Bus4 has the highest absolute fault-current magnitude, while Bus5 and Bus6 exhibit more persistent DC-offset behavior. Therefore, equipment specification should consider both symmetrical fault current and asymmetrical/momentary duty. Protection coordination should subsequently be developed using the fault levels under relevant network configurations, including future distributed-energy-resource scenarios.

3.8 ENGINEERING IMPLICATIONS AND IMPLEMENTATION PRIORITIES

The simulation results support a staged implementation strategy. First, assess reactive-power support at the 33 kV point of common coupling to improve source power factor and reduce reactive losses. Second, prioritize the Ifite and Industrial feeders for capacity review or load redistribution because they are the most stressed circuits. Third, introduce smart monitoring, automated switching/reclosing, feeder fault indication, and transformer condition monitoring to improve visibility and response. Fourth, verify the interrupting and short-time ratings of the switchgear around Bus6 and the 33 kV buses against the simulated fault-duty envelope and complete the relay coordination study when verified settings are available. Finally, develop an alternative 11 kV supply path, additional firm transformer capacity, or coordinated load-transfer/load-shedding scheme before full deployment.

3.9 LIMITATIONS

This study is simulation-based and is limited by the availability of verified utility operating records and by access to advanced ETAP modules. Some parameters were taken from standard references, ETAP libraries, manufacturer information, or engineering assumptions where utility records were unavailable. The proposed IEC 61850 communication and edge-processing specifications are design proposals, not measurements from a deployed digital substation. Likewise, the paper does not claim completed field validation, relay TOC coordination, breaker-rating verification, or measured post-upgrade performance. These items require utility data and detailed equipment records and are identified as next-stage work.

4.0. Conclusion

This paper has presented an ETAP-based smart-substation design and reliability assessment for the Agu Awka 33/11 kV injection substation. The modeled network converged successfully in the base case, with 18.467 MW and 6.070 Mvar of demand and 0.277 MW and 1.958 Mvar of losses. Although the bus voltages remained within the ±5% band, the downstream voltage profile declined to approximately 95.21–95.80% at the feeder buses. All four feeders were modeled at approximately 102.7–103.1% of their stated ratings, while the two 33 kV sources operated at 91.92% power factor.

The short-circuit assessment identified the 0.415 kV auxiliary bus as the location with the highest initial symmetrical fault current and Bus6 as a critical 11 kV fault-duty location. The contingency analysis showed that Bus6 is the dominant N-1 vulnerability and that the network has essentially no practical N-2 margin under the studied conditions. These results establish that smart-substation modernization should combine digital automation with physical reinforcement, reactive-power support, protection-duty verification, and improved supply-path redundancy.

The principal contribution is therefore an integrated, simulation-grounded framework for assessing a medium-voltage smart injection substation in a developing-country distribution context. The approach can be extended to adaptive protection, distributed generation, quantitative reliability indices, cyber-resilience assessment, and field validation.

5.0 Recommendation

Future work should proceed in five linked stages. First, obtain time-synchronized SCADA and substation-meter records and use them to calibrate and independently validate the ETAP model under representative operating conditions.

Second, complete a formal relay coordination study using verified CT ratios, relay pickup settings, time-current characteristics, breaker operating times, and manufacturer interrupting and short-time withstand ratings. The simulated symmetrical and asymmetrical fault currents reported in this paper should form the initial duty envelope for that study.

Third, develop the proposed IEC 61850 digital layer as a detailed engineering design, including device selection, GOOSE/SV/MMS traffic engineering, IEEE 1588-time synchronization, network redundancy, cybersecurity controls, and edge-node acceptance tests.

Fourth, investigate physical reinforcement measures, including feeder capacity upgrades, additional firm transformer capacity, an alternative 11 kV supply path, and coordinated load transfer or automatic load shedding. Reactive-power compensation should be optimized with voltage, loss, and harmonic constraints.

Finally, extend the assessment to distributed-energy-resource integration, adaptive protection, quantitative reliability indices, cyber-resilience testing, and comparative before-and-after field performance.

Acknowledgements

The authors acknowledge the assistance and support of the Chief Technical Officer, First Power Electricity Distribution Company (FPEDC), Corporate Headquarters, Awka, Anambra State, for providing materials and data used in this research.

Declaration of Generative AI and AI-assisted technologies in the writing process

During the preparation of this work the author(s) used ChatGPT tool in order to generate the conceptual transition from conventional to smart injection-substation architecture and the proposed smart-substation architecture showing process/bay/station functions, SCADA, RTU, IEDs, sensors, automated breakers/reclosers, and communication links shown in Figures 1 and 3 only. It was also used for language editing, and structural refinement. The rest of the information on the article are original work of the authors. After using this tool/service, the author(s) reviewed and edited the content as needed and take(s) full responsibility for the content of the publication.

References

Cabral, E. A., Melo, B. V., Tofoli, F. L., Sampaio, R. F., & Leão, R. P. S. 2026. Modeling and assessment of digital substations based on IEC 61850 standard: An integrated approach to security and industry 4.0 resources using the system-theoretic process analysis method. Electric Power Systems Research, 259, 113213. https://doi.org/10.1016/j.epsr.2026.113213

Chen, Z., Amani, A. M., Yu, X., & Jalili, M. 2023. Control and optimisation of power grids using smart meter data: A review. Sensors, 23(4), 2118. https://doi.org/10.3390/s23042118

El-Fergany, A. A. 2024. Reviews, challenges, and insights on computational methods for network reconfigurations in smart electricity distribution networks. Archives of Computational Methods in Engineering, 31, 1233–1253. https://doi.org/10.1007/s11831-023-10007-0

Girdhar, M., Park, K., Su, W., Hong, J., Herath, A., & Liu, C. 2024. SDN-based smart cyber switching (SCS) for cyber restoration of a digital substation. arXiv preprint arXiv:2411.07433. https://doi.org/10.48550/arXiv.2411.07433

Glover, J. D., Overbye, T. J., & Sarma, M. S. 2017. Power system analysis and design (6th ed.). Cengage Learning.

Heluany, J. B., & Gkioulos, V. 2024. A review on digital twins for power generation and distribution. International Journal of Information Security, 23, 1171–1195. https://doi.org/10.1007/s10207-023-00784-x

Husnoo, M. A., Anwar, A., Hosseinzadeh, N., Islam, S. N., Mahmood, A. N., & Doss, R. 2023. False data injection threats in active distribution systems: A comprehensive survey. Future Generation Computer Systems, 140, 344–364. https://doi.org/10.1016/j.future.2022.10.021

IEC 61850-7-2. 2020. Communication networks and systems for power utility automation—Part 7-2: Basic information and communication structure—Abstract communication service interface (ACSI). International Electrotechnical Commission.

IEC 61850-8-1. 2020. Communication networks and systems for power utility automation—Part 8-1: Specific communication service mapping (SCSM)—Mappings to MMS and ISO/IEC 8802-3. International Electrotechnical Commission.

IEC TR 61850-90-4. 2020. Communication networks and systems for power utility automation—Part 90-4: Network engineering guidelines. International Electrotechnical Commission.

Mathebula, V. C., & Saha, A. K. 2022. Reliability of IEC 61850 based substation communication network architecture considering quality of repairs and common cause failures. Protection and Control of Modern Power Systems, 7, 13. https://doi.org/10.1186/s41601-022-00234-1

Moradi-Sepahvand, M., Amraee, T., Aminifar, F., & Akbari, A. 2023. Coordinated expansion planning of transmission and distribution systems integrated with smart grid technologies. International Journal of Electrical Power & Energy Systems, 147, 108859. https://doi.org/10.1016/j.ijepes.2022.108859

Ratshitanga, M., Orumwense, E. F., Krishnamurthy, S., & Melamu, M. 2023. A review of demand-side resources in active distribution systems: Communication protocols, smart metering, control, automation, and optimization. Applied Sciences, 13(23), 12573. https://doi.org/10.3390/app132312573

Roomi, M. M., Hussain, S. M. S., Chang, E.-C., Nicol, D. M., & Mashima, D. 2025. Auto-SGCR: Automated generation of smart grid cyber range using IEC 61850 standard models. IEEE Open Journal of the Industrial Electronics Society, 6, 1575–1592. https://doi.org/10.1109/OJIES.2025.3604576

Zhu, M., Liang, M., Li, H., Lu, Y., & Pang, M. 2023. Intelligent acceptance systems for distribution automation terminals: An overview of edge computing technologies and applications. Journal of Cloud Computing, 12, 149. https://doi.org/10.1186/s13677-023-00529-0

IEC 60909-0. 2026. Short-circuit currents in three-phase AC systems—Part 0: Calculation of currents. International Electrotechnical Commission.